

A Review of Wavelets in Biomedical Applications

MICHAEL UNSER, SENIOR MEMBER, IEEE, AND AKRAM ALDROUBI

Invited Paper

In this paper, we present an overview of the various uses of the wavelet transform (WT) in medicine and biology. We start by describing the wavelet properties that are the most important for biomedical applications. In particular, we provide an interpretation of the continuous wavelet transform (CWT) as a prewhitening multiscale matched filter. We also briefly indicate the analogy between the WT and some of the biological processing that occurs in the early components of the auditory and visual system. We then review the uses of the WT for the analysis of 1-D physiological signals obtained by phonocardiography, electrocardiography (ECG), and electroencephalography (EEG), including evoked response potentials. Next, we provide a survey of recent wavelet developments in medical imaging. These include biomedical image processing algorithms (e.g., noise reduction, image enhancement, and detection of microcalcifications in mammograms), image reconstruction and acquisition schemes (tomography, and magnetic resonance imaging (MRI)), and multiresolution methods for the registration and statistical analysis of functional images of the brain (positron emission tomography (PET) and functional MRI (fMRI)). In each case, we provide the reader with some general background information and a brief explanation of how the methods work.

I. INTRODUCTION

In the past few years, researchers in applied mathematics and signal processing have developed powerful wavelet methods for the multiscale representation and analysis of signals [22], [104]. These new tools differ from the traditional Fourier techniques by the way in which they localize the information in the time-frequency plane; in particular, they are capable of trading one type of resolution for the other, which makes them especially suitable for the analysis of nonstationary signals. One privileged area of applications where these properties have been found to be relevant is biomedical engineering.

Due to the wide variety of signals and problems encountered in medicine and biology, the spectrum of applications of the wavelet transform (WT) has been extremely large. It ranges from the analysis of the more traditional physiological signals such as the electrocardiogram (ECG), to the very recent imaging modalities including positron emission

tomography (PET) and magnetic resonance imaging (MRI). The main difficulty in dealing with biomedical objects is the extreme variability of the signals and the necessity to operate on a case by case basis. Often, one does not know *a priori* what is the pertinent information and/or at which scale it is located. For example, it is frequently the deviation of some signal feature from the normal that is the most relevant information for diagnosis. As a result, the problems tend to be less well defined than those in engineering and the emphasis is more on designing robust methods that work in most circumstances, rather than procedures that are optimal under very specific assumptions. Another important aspect of biomedical signals is that the information of interest is often a combination of features that are well localized temporally or spatially (e.g., spikes and transients in electroencephalograph (EEG) signals and microcalcifications in mammograms) and others that are more diffuse (e.g., small oscillations, bursts, and texture). This requires the use of analysis methods sufficiently versatile to handle events that can be at opposite extremes in terms of their time-frequency localization.

The purpose of this paper is to review the various uses of the WT and the corresponding research efforts in the biomedical area. The presentation is organized around two main axes: 1) a discussion of the main properties of the WT and their particular relevance for biomedical problems (the point of view of the wavelet expert) and 2) a critical review of the applications classified by biomedical subjects (the point of view of the biomedical specialist). In Section II, we start by examining the properties of the WT that are the most relevant to medicine and biology, with the help of many illustrative examples. This material is provided as a complement to the more general introduction to the WT given in [20]. In Section III, we consider the primary 1-D biomedical signal processing applications (bioacoustics, ECG, and EEG), providing the reader with the relevant background, and reviewing the recent wavelet developments in those areas. In Section IV, we consider the applications of wavelets to biomedical imaging. These include image processing tasks (noise reduction, enhancement, and detection), reconstruction and acquisition techniques for X-ray tomography and MRI, and

Manuscript received June 1, 1995; revised December 15, 1995.

The authors are with the Biomedical Engineering and Instrumentation Program, National Center for Research Resources, National Institutes of Health, Bethesda, MD 20892-5766 USA.

Publisher Item Identifier S 0018-9219(96)02350-X.

statistical methods for localizing patterns of activity in the brain using functional imaging (PET and fMRI).

This whole area of research is still relatively new, but is evolving very rapidly. Our bibliography includes most of the papers that had appeared in refereed journals prior to May 1995, plus a limited number of preprints of which we were aware. To enlarge the coverage, we also considered a limited number of published conference papers. Although we did our best to provide the most complete overview within the given constraints, we apologize in advance to those authors whose work was been left out of the discussion.

Beside the growing number of researchers and the rate of publication that keeps increasing steadily, there are other indicators of the current popularity of wavelets in biomedical engineering. The first event that was entirely devoted to this subject was the workshop on Wavelets in Medicine and Biology, which was part of the 1994 *IEEE-EMBS* conference in Baltimore. There have also been two special issues of the *IEEE Engineering in Medicine and Biology Magazine*: one on time-frequency and wavelet analysis of biomedical signals which appeared in March/April 1995, and one on wavelets for image analysis scheduled for October 1995. Finally, there is a textbook to be published shortly on the subject that should provide an additional source of information [7].

II. WAVELET PROPERTIES IN THE CONTEXT OF BIOMEDICAL APPLICATIONS

This section is intended to complement the general introduction to the WT that is given in [20]. Its purpose is to reexamine some of its properties in relation to biomedical applications. From the point of view of the practitioner, there are essentially two types of wavelet decomposition: the redundant ones (continuous wavelet transform (CWT) or wavelet frames), and the nonredundant ones (orthogonal, semi-orthogonal, or biorthogonal wavelet bases). The first type is usually preferable for signal analyses, feature extraction, and detection tasks for it provides a description that is truly shift-invariant; the wavelet properties that are of special interest for this class of applications are discussed in Sections II-A–C. The second type, which is discussed in Section II-D, is obviously more nearly adequate whenever it is desirable to perform some kind of data reduction, or when the orthogonality of the representation is an important factor. However, the choice between these two options is not necessarily clear-cut because of computational considerations. A decomposition in terms of wavelet bases using Mallat's fast algorithm is typically orders of magnitude faster than a redundant analysis, even if one uses the fastest available algorithms [83], [98]. For the first class of problems, there is a cost benefit trade-off, and many researchers have considered nonredundant wavelet decompositions and obtained very satisfactory results.

A. Wavelets as a Filterbank

For a fixed value of the scale parameter a , the WT which is now a function of the continuous shift parameter b , can

be rewritten as a convolution equation

$$T_\psi f(a = \text{Const}, b) = \langle f, \psi_{(a,b)} \rangle = (f * \bar{\psi}_a^T)(b) \quad (1)$$

where the filtering template $\bar{\psi}_a^T(x) = a^{-1/2}\bar{\psi}(-x/a)$ corresponds to a rescaled and time-reversed version of the wavelet $\psi(x)$. The frequency response of this filter is simply $a^{1/2}\hat{\bar{\psi}}(a\omega)$, where $\hat{\bar{\psi}}$ is the complex conjugate of Fourier transform of ψ . Thus if we evaluate (1) for a discrete set of scales (for example, the dyadic values 2^i), we obtain what is frequently referred to as a constant- Q filterbank.¹ This type of analysis provides a decomposition of a signal into subbands with a bandwidth that increases linearly with the frequency. In the case of a dyadic transform, each spectral band is approximately one octave wide [Fig. 1(a)]. In this form, the WT can be viewed as a special kind of spectral analyzer. The simplest global features that can be extracted from this type of system are energy estimates in the various bands or other related measures. Spectral features of this type have been used recently to discriminate between various physiological states. Two examples are the analysis of turbulent heart sounds to detect coronary artery disease [5] and the characterization of states of fetal electrocortical activity [2]. We should note, however, that this type of global feature extraction is only justified when the underlying signal can be assumed to be stationary and that similar results can also be obtained using more conventional Fourier techniques.

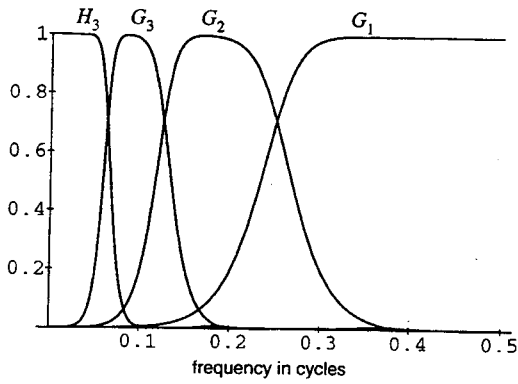
If the transfer functions of the discrete filters associated with a redundant m channel dyadic wavelet decomposition are denoted by $G_1(\omega), \dots, G_{m-1}(\omega), H_m(\omega)$, where $G_i(\omega) \cong \hat{\psi}(2^i\omega)$ and $H_m(\omega)$ is a suitable lowpass filter, then it is possible to obtain a corresponding reconstruction algorithm if the synthesis filters in Fig. 1(b) are chosen such that

$$H_m(\omega)\tilde{H}_m(\omega) + \sum_{i=1}^{m-1} G_i(\omega)\tilde{G}_i(\omega) = 1 \quad (2)$$

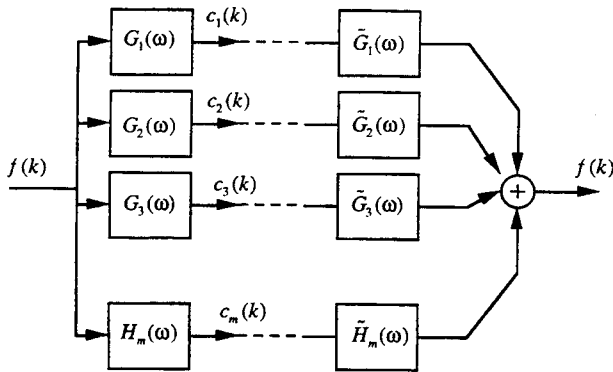
i.e., the system acts globally as the identity. If the wavelet $\psi(x)$ is derived from a multiresolution analysis, then the corresponding filterbank can be implemented by using an adapted ("à trous") version of Mallat's fast algorithm without subsampling [59], [99]. This type of reversible wavelet decomposition can be the basis for the implementation of noise reduction and image enhancement algorithms (Section IV-A). The principle is to insert an additional processing component that selectively modifies the wavelet components prior to reconstruction.

Mallat and Zhong also used such a filterbank system to obtain a multiscale edge representation of a signal from its wavelets maxima [60]. They proposed an iterative algorithm that reconstructs a very close approximation of the original from this subset of features. This approach has been adapted for noise reduction in evoked response potentials (Section III-C), as well as MR images (Section IV-C).

¹The Q -factor is defined as the central frequency to bandwidth ratio; it is a constant for a wavelet-type analysis.



(a)



(b)

Fig. 1. Wavelets as a filterbank. (a) Multiband frequency response of the discrete filterbank associated with the cubic spline Battle-Lemarié wavelets. (b) Discrete perfect reconstruction filterbank without subsampling.

B. Wavelets as a Multiscale Matched Filter

In essence, the CWT performs a correlation analysis, so that we can expect its output to be maximum when the input signal most resembles the analysis template $\psi_{(a,b)}$. This principle is the basis for the matched filter, which is the optimum detector of a deterministic signal in the presence of additive noise.

Consider the measurement model $f(x) = \varphi_a(x - \Delta x) + n(x)$ where $\varphi_a(x) = \varphi(x/a)$ is a known deterministic signal at scale a , Δx an unknown location parameter, and $n(x)$ an additive white Gaussian noise component. Classical detection theory tells us that the optimal procedure for estimating Δx is to perform the correlation with all possible shifts of our reference template (convolution) and to select the position that corresponds to the maximum output (maximum likelihood solution). Therefore, it makes sense to use a WT-like detector whenever the pattern φ that we are looking for can appear at various scales.

If the noise is correlated instead of white, then we can get back to the previous case by applying a whitening filter. This leads to the prewhitening matched filter whose frequency response is $\tilde{\varphi}_a(\omega)/\phi_n(\omega)$, where $\phi_n(\omega)$ is the noise power spectral density [115]. Strickland presents a case where the corresponding detector closely resembles a WT [92]. Here we take the argument one step further and show that the wavelet-like structure of the detector is

preserved exactly if the noise has a fractional brownian motion structure. Specifically, if the noise average spectrum has the form $\phi_n(\omega) = \sigma^2/|\omega|^\alpha$ with $\alpha = 2H + 1$ where H is the Hurst exponent, it is not difficult to establish that the optimal prewhitening matched filter at scale a is

$$(-j)^\alpha D^\alpha \varphi_a(x) = C_a \cdot \psi(x/a) \quad (3)$$

where $j = \sqrt{-1}$ and where D^α is α th fractional derivative operator (multiplication by $(j\omega)^\alpha$ in the Fourier domain). In other words, the (real-valued) wavelet $\psi(x)$ is proportional to the fractional derivative of the pattern φ that we want to detect. Consequently, for $H > 0$, the optimal detector is an admissible wavelet even if the initial template $\varphi(x)$ is not (e.g., it is a lowpass function). For example, the optimal detector for finding a Gaussian in $O(\omega^{-2})$ noise is the Mexican hat wavelet (second derivative of a Gaussian). As suggested by Strickland's analysis [92], this is perhaps one of the main reasons why the WT works well for detecting microcalcifications in mammograms (Section IV-A).

The detection properties of the WT have also been used advantageously for certain biomedical signal processing tasks. One example is the detection of interictal spikes in EEG recordings of epileptic patients (Section III-C). There are also applications in cardiology (Section III-B), for example, the detection of the QRS complex in ECG signals [52]. We should note that this last application also exploits the ability of the WT to characterize singularities through the decay of the wavelet coefficients across scale [20, Section 2].

C. Wavelets and Time-Frequency Localization

The function that has the best time-frequency localization in the sense specified by the uncertainty principle is the Morlet or Gabor wavelet $\psi(x) = e^{j\omega_0 x} e^{-x^2/2}$. The corresponding analysis template $\psi_{(a,b)}$ is centered at the position $x = b$ and the standard deviation of its Gaussian envelope is $\sigma_x = a$. Its Fourier transform is a Gaussian as well, with a central frequency $\omega = \omega_0/a$ and a standard deviation $\sigma_\omega = a^{-1}$. Thus each analysis template tends to be predominantly located in a certain elliptical region of the time-frequency plane; the same qualitative behavior also applies for other nongaussian wavelet functions. Note that the area of these localization regions is the same for all templates and that it is constrained by the uncertainty principle. Thus by measuring the correlation between the signal and each wavelet template, we obtain a characterization of its time-frequency content (scalogram). Its main difference with the short-time Fourier transform is that the size of the analysis window is not constant for it varies in inverse proportion to the frequency (i.e., $a = \omega_0/\omega$ where ω_0 is the central wavelet frequency). This property enables the WT to zoom in on details, but at the expense of a corresponding loss in spectral resolution. Since we cannot simultaneously achieve a good localization in time and frequency, the name of the game in time-frequency analysis is to trade one type of localization for the other in a way that is well adapted to the characteristics of the input signal. In this respect, we should note that most biomedical signals of interest include a combination of impulse-like events (spikes and

transients) and more diffuse oscillations (murmurs and EEG waveforms) which may all convey important information for the clinician. The short-time Fourier transform or other conventional time-frequency methods are well adapted for the latter type of events but are much less suited for the analysis of short duration pulsation. When both types of events are present in the data, the WT can offer a better compromise in terms of localization. This may explain its success in biomedical signal processing. Recent examples of applications where time-frequency wavelet analysis appears to be particularly appropriate are the characterization of heart beat sounds [46], [45], [69], the analysis of ECG signals including the detection of late ventricular potentials [45], [30], [68], [90], the analysis of EEG's [89], [88], [43], as well as a variety of other physiological signals [87].

The Gabor-Morlet wavelet cannot generate a basis of L_2 and are only appropriate for performing a redundant wavelet analysis. Yet, it is also possible to construct semi-orthogonal wavelet bases with a time-frequency that is arbitrarily close to the limit specified by the uncertainty principle [8]. This property was first demonstrated with the B-spline wavelets which converge to a cosine-Gabor function as the degree of the spline goes to infinity [100]. In practice, it is sufficient to chose a cubic B-spline wavelet [Fig. 2(b)], which provides a localization that is already within a few percent of the limit specified by the uncertainty principle. The advantage of these wavelets is that they can be implemented very efficiently using standard decimated (or nondecimated) filterbank algorithms.

D. Wavelet Bases

Perhaps the most remarkable aspect of wavelet theory is the possibility to construct wavelet bases of L_2 (the spaces of square integrable functions) [62], [21]. The wavelet basis is generally given by the set of dilated (index i) and translated (index k) versions of the mother wavelet $\{\psi_{i,k} = 2^{-i/2}\psi(x/2^i - k)\}_{(i,k) \in \mathbb{Z}^2}$. Hence, it is possible to represent a signal through its wavelet expansion

$$f = \sum_i \sum_{k \in \mathbb{Z}} c_{i,k} \psi_{i,k} \quad (4)$$

where the wavelet coefficients $c_{i,k}$ are obtained through the following inner product

$$c_{i,k} = \langle f, \tilde{\psi}_{i,k} \rangle. \quad (5)$$

The function $\tilde{\psi}$ is the dual analysis wavelet; in the orthogonal case, ψ and $\tilde{\psi}$ are identical. In addition, associated with such a decomposition is a fast filterbank decomposition algorithm [63], [20].

The important point for our purpose is that, in the discrete case, the decomposition formula (4) provides a one-to-one representation of the signal in terms of its wavelet coefficients (reversible linear transformation). Data compression as well as noise reduction can be achieved by quantization in the wavelet domain, or by simply discarding certain coefficients that are insignificant (Sections III-C and IV-A).

This form of orthogonal (or close-to-orthogonal) wavelet decomposition was found to be very useful for image coding [51], [10], [28], [91]. There have also been specific

applications of wavelet compression to medical images, including MR images [9], digital mammograms [56], as well as full 3-D data sets [64], [13], [65]. One should note, however, that the use of lossy image compression schemes for medical images is still controversial. One of the problems is that the usual, nonmedical image quality criteria are not necessarily very meaningful in the context of diagnostic radiology. The use of these techniques also raises some delicate legal issues.

While the future of medical image compression remains unclear, the availability of multiresolution wavelet bases has probably had the greatest impact on some of the more fundamental aspects of medical imaging, including tomographic reconstruction, image acquisition, and functional imaging. These various applications, which are described in Section IV, all take advantage of the property that the wavelet basis functions retain a certain degree of localization in space.

In addition to the multiresolution wavelet bases, we should also mention wavelet packets, which produce more general tilings of the time-frequency plane. The most appropriate transform within the given family is usually found by optimizing an application-dependent criterion (best basis algorithm). Karatchouc *et al.* introduced a correlation criterion to configure an adaptive subband filtering algorithm for respiratory interference cancelation in pulmonary capillary pressure [44]. Healy and Weaver also considered wavelet packet solutions for MRI encoding [109], [40] (Section IV-C).

E. Wavelets as a Model of Perception

Interestingly, there is a striking similarity between the WT and some of the biological information processing that occurs in the first stages of auditory and visual perception [107], [61]. This has led various authors to propose wavelet-like models for low-level auditory and visual sensory processing.

1) *The Auditory System:* The analysis of acoustic signals in the brain involves two main functional components: 1) the early auditory system which includes the outer ear, middle ear, inner ear (the cochlea), and the cochlear nucleus and 2) the central auditory system, which consists of a highly organized network of neurons in the cortex. When a sound pressure $p(t)$ impinges on the outer ear, it is transmitted to the inner ear, transduced into neural electrical impulses, which are further transformed and processed in the central auditory system. The preprocessing and analysis of sounds in the early and central systems involve a series of processes best modeled by nonlinear dynamics [35], [106], [114], [41]. However, both systems include linear processing stages that behave like WT's. In particular, it has been shown that the snail-like cochlea transforms the acoustic pressure $p(t)$ received from the middle ear, into displacements $y(t, x_1)$ of its basilar membrane given by the convolution equation [114], [107]

$$y(t, x_1) = (p(\cdot) * h(\cdot, x_1))(t) \quad (6)$$

where x_1 is a curvilinear coordinate along the cochlea, c a propagation velocity, and where $h(t, x_1) = h(ct/x_1)$ is

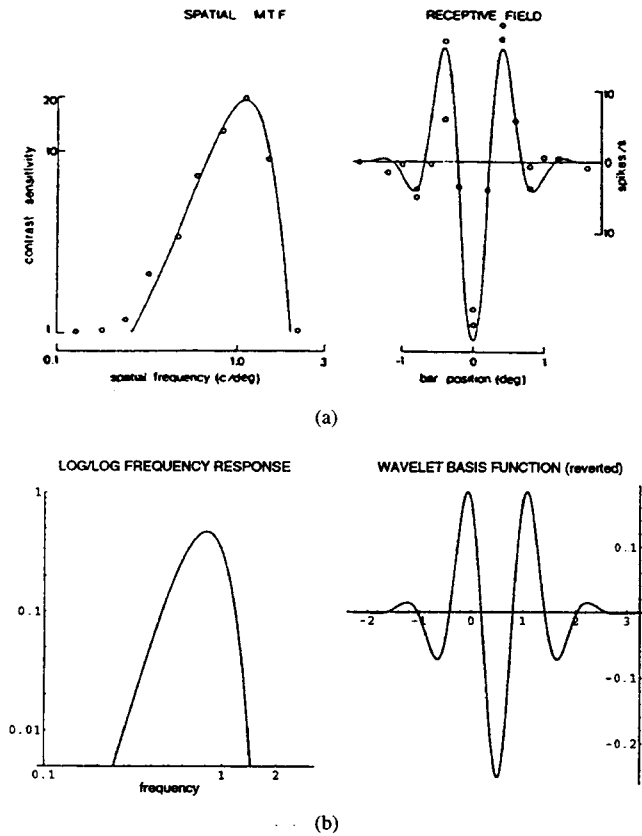


Fig. 2. Similarity between the receptive field of simple cortical cells and a wavelet basis function. (a) Response of a simple X cell from a monkey visual cortex and its fitted Gabor elementary signal [26], [67, Fig. 3]. (b) Semi-orthogonal cubic B-spline wavelet and its log-log frequency response [100].

the cochlear bandpass filter located at x_1 . Thus $y(t, x_1)$ is simply the CWT of $p(t)$ with the wavelet $h(t)$ at a time scale proportional to position x_1/c . This property has also inspired new engineering applications for the detection, transmission, and coding of auditory signals [14].

2) *Visual System*: Even though the primary visual cortex has many other complex functional units, it includes an important population of neurons that have wavelet-like properties. These are the so-called *simple cells* of the occipital cortex, which receive information from the retina through the lateral geniculate nucleus and send projections to the complex and hypercomplex cells of the primary and associative visual cortices. The receptive fields of these cells (i.e., the corresponding area on the retina that produces a response) consist of distinct elongated excitatory and inhibitory zones of a given size and orientation and their response is approximately linear [42]. Simple cortical cells have also been characterized by their frequency response which is a directional bandpass, with a radial bandwidth that is more or less proportional to the central frequency (constant- Q analysis) [25]. Another remarkable feature is the topographic organization of these neurons into "columns" which share a common preferential orientation (not unlike wavelet channels). Marcelja showed that the spatial responses of individual cells are well represented

by modulated Gaussians [67]. Note the striking similarity between the cell's response² in Fig. 2(a) adapted from [67], and the cubic B-spline wavelet basis function mentioned previously [Fig 2(b)]. Considerations of this nature led researchers to formulate a variety of multichannel neuronal models consisting of a set of directional Gabor filters with a hierarchical wavelet-like organization [23], [24], [108], [77]. Simpler decompositions in terms of wavelet-basis have also been considered [34].

III. BIOMEDICAL SIGNAL PROCESSING

Having reviewed the principal properties of the WT, we now proceed with a more detailed overview by biomedical subject. We start with the primary physiological signals (1-D processing).

A. Bio-Acoustics

The pumping of the heart gives rise to mechanical vibrations that can be perceived as pulses or sound through a stethoscope. Better quality recordings of these sounds can be obtained by placing a microphone inside the heart via a catheter or within the esophagus using a tube. The analysis of heart sounds can provide valuable insights into the course of cardiac activity, even though this diagnostic method is progressively being taken over by ultrasound. The auditory events of the heart are classified into heart sounds and murmurs. Sounds are short, impulse-like events that represent transitions between the different hemodynamic phases of the cycle. Murmurs, which are primarily caused by blood flow turbulence, are characteristic of cardiac disease such as aortic stenosis, or valve defects. These are distributed over the whole cycle. The sound induced by stenosis will typically be the loudest during systole where the blood flow is maximum.

Khadra *et al.* were the first to suggest that the WT can provide a useful tool for the time-frequency analysis and characterization of the primary heart sounds [46]. Its adequacy for this particular application was further confirmed in a comparative study with other time-frequency methods (Wigner distribution and spectrogram) [69]. In particular, Obaidat showed that the WT could pick up certain sound components (e.g., the aortic and pulmonary valve components of the second heart sound) that could not be resolved by the other methods. Akay *et al.* considered the analysis of the more diffuse turbulent sounds. In particular, they used simple global wavelet statistics to investigate the effects of vasodilator drugs on the turbulent sounds caused by arterial stenosis [2]. The same type of wavelet features were also used in a classification experiment that was aimed at detecting subjects with coronary artery disease in a group of 122 patients [5].

Interestingly, these recent wavelet methods are reminiscent of the analog octave filter bank proposed by Mannheimer in 1942 to extract the various components of the phonocardiographic signal [66]. This filter, which used to be an integral part of heart sound amplification systems, enabled the experimenter to isolate faint components such

²The data presented corresponds to the spatial and spatial-frequency measurements performed by De Valois *et al.* [26].

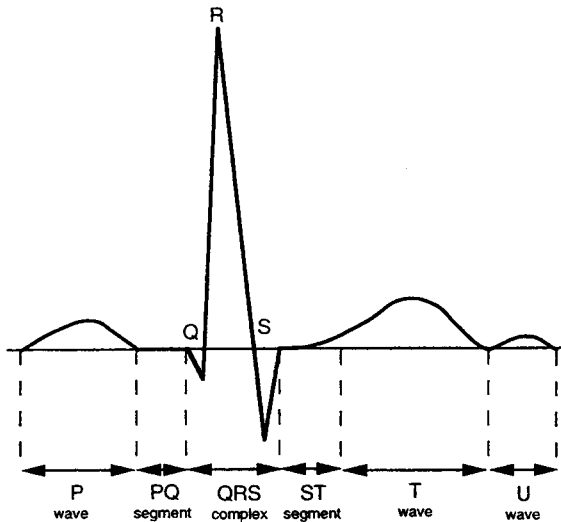


Fig. 3. Schematic representation and labeling of the ECG (one cardiac cycle).

as heart murmurs that could not have been picked out otherwise (masking effect of the high amplitude low frequency components).

B. Electrocardiography (ECG)

The ECG signal represents the changes in electrical potential during the cardiac cycle as recorded between surface electrodes on the body. The characteristic shape of this signal is the result of an action potential that propagates within the heart and causes the contraction of the various portions of the cardiac muscle. This internal excitation starts at the sinus node which acts as a pacemaker, and then spreads to the atria; this generates the characteristic P wave in the ECG (Fig. 3). The cardiac excitation then reaches the ventricles (ventricular depolarization) giving rise to the characteristic QRS complex. Once the ventricles have been completely stimulated (ST segment of the ECG), they repolarize corresponding to the T wave of the ECG. The automatic detection and timing of these waves is important for diagnostic purposes.

The crucial step in the analysis of ECG is the detection of the QRS complex. While there are many other algorithms available, there has been a recent proposal for a wavelet-based approach which provides excellent performance (a detection of 99.8% for the MIT/BIH arrhythmia database) [53]. Senhadji *et al.* have demonstrated the potential of wavelet-based feature extraction for discriminating between normal and abnormal cardiac patterns [90]. The WT has also been applied to the detection of ventricular late potentials (VLP) [97], [45], [30], [68]. These are small signals with a frequency content above 40 Hz, which have been associated with coronary heart disease, myocardial infarctions, and ventricular arrhythmia. VLP's are typically found in the terminal part of the QRS complex and in the beginning of the ST segment, but they can also occur during the whole QRS complex. While other time-frequency methods can also be used for this task, the results

of Khadra and Dickau suggest that the detection accuracy of the WT is superior [45], [30].

Wavelets were also applied to characterize beat-to-beat fluctuations of the heart rate under varying physiological conditions [3], [96]. However, their advantages over the more standard spectral analysis techniques remains to be demonstrated [6].

C. Electroencephalography (EEG)

The synchronous discharge of nerve cells creates rhythmic potential fluctuations on the head surface, which can be measured through electroencephalography. Even if the method is relatively ancient (1924), the electroencephalogram (EEG) is still considered an important clinical tool in neurosurgery, psychiatry, and pediatrics.

1) *Seizure Detection:* EEG is especially important for the diagnosis of epilepsy. One of the early sign of a seizure is the presence of characteristic transient waveforms in the EEG (spikes and sharp waves). As the seizure progresses, the transient activity slowly develops into more nearly regular high amplitude quasiperiodic oscillations, reflecting abnormal discharge of a large group of neurons. The shape and size of these waveforms can vary substantially from one patient to the other. Here again, the WT appears to be an appropriate detection tool due to the very mixed nature of these phenomena. This has been first demonstrated in the case of intracranial EEG, where electrodes are implanted directly on the surface of the brain in order to localize seizures for neurosurgery [89], [88]. Real time processing is very desirable in this context and fast CWT algorithms were developed with that objective in mind [102], [88]. With scalp EEG, the detection task is more difficult because of signal attenuation and the presence of interfering background noise (electromyogenic activity). The WT may still provide a valuable feature extraction tool, as suggested by the classification experiments of Kalayci and Ozdamar who trained a neural network to discriminate between two classes of signals: 1) short abnormal EEG segments with a spike in the center (with or without sharp wave complexes) and 2) others corresponding to any other form of activity [43].

Another related application of the WT is the analysis of fetal electrocortical activity using implanted brain electrodes [1]. So far, most efforts have been directed toward the simpler discrimination tasks where the problem is to distinguish between different patterns of global activity; e.g., high voltage slow activity versus low voltage fast activity. This methodology has also been used to assess the effect of opioid drugs on brain activity [4].

2) *Evoked Potentials:* The sensitivity of electroencephalography can be dramatically improved by looking at evoked response potentials (ERP's). This method creates perturbations in the EEG using an external acoustic, visual, or somatosensory stimulus. The latency from the time of stimulation is used to distinguish between electrical events that directly reflect the characteristics of the stimulus (latency <100 ms) or those that reflect cognitive processing (latency >100 ms). ERP's are usually acquired using multiple synchronized trials (typically

100–600 repetitions) and noise reduction is achieved through ensemble averaging.

Thakor *et al.* characterized the shape of partially averaged somatosensory ERP's using global wavelet energies and showed that these measures provided a reliable tracking of the time course of neurologic injury (cerebral hypoxia) [93]; comparable results could also be obtained using Fourier-based descriptors.

Depending on the number of trials, there may still be some residual noise after ensemble averaging. The measurement model in this case is a deterministic signal (ERP) plus noise (residual EEG) which may be assumed to be stationary. An elegant approach for noise reduction proposed by Bertrand *et al.* is to perform a generalized Wiener filtering in the wavelet domain [16]. In this particular application, the WT appears to be superior to the Fourier transform, the latter being optimal only when both the signal and noise are stationary (conventional Wiener filter). Lim *et al.* also report good noise reduction results with respiratory-related ERP's by simply discarding the three upper wavelet bands [54], which also corresponds to a particular form of wavelet filtering. The benefit of these techniques is a possible reduction of the number of trials, the ultimate goal being to extract the ERP using no averaging at all. One proposal is to reconstruct single ERP's from a reduced number of wavelet coefficients [12], [17], which again falls into the same filtering framework. In this method, the selection of the significant coefficients is based on a discriminant analysis between the signal + noise and noise-only (ongoing EEG) recordings. Carmona and Hudgins considered a completely different approach and attempted to reduce noise in ERP's using Mallat and Zhong nonlinear denoising algorithm which reconstructs the signal from its wavelet maxima [18].

IV. BIOMEDICAL IMAGING

Many of the 1-D applications reviewed so far used wavelet techniques that are not necessarily specific to biomedical signals. We will see that the situation in 2-D is different. Except for some of the image processing methods described in Section IV-A, the wavelet techniques developed for medical imaging are quite specific and appear to have no equivalent in nonbiomedical applications.

A. Biomedical Image Processing

1) *Noise Reduction*: One of the first application of the WT in medical imaging was for noise reduction in MR images [110]. The approach proposed by Weaver *et al.* was to compute an orthogonal wavelet decomposition of the image and apply the following soft thresholding rule on the coefficients $c_{i,k} = \langle f, \psi_{i,k} \rangle$

$$\tilde{c}_{i,k} = \begin{cases} c_{i,k} - t_i & c_{i,k} \geq t_i \\ 0 & |c_{i,k}| \leq t_i \\ c_{i,k} + t_i & c_{i,k} \leq -t_i \end{cases} \quad (7)$$

where t_i is a threshold that depends on the noise level at the i th scale; the image is then reconstructed by the inverse WT of the $\tilde{c}_{i,k}$'s. This is essentially the wavelet

shrinkage denoising method later systematized by Donoho and Johnston [31]–[33], as well as DeVore and Lucier [29]. A more sophisticated approach uses an overcomplete wavelet decomposition and a variation of the Mallat and Zhong algorithm [60] to reconstruct the image from its wavelet maxima [113]. The significant wavelet maxima are retained by exploiting the correlation between adjacent scales. When applied to MR images, the method compared quite favorably with the optimal space-invariant solution (Wiener filter); in particular, it produced images with much sharper edges and did not induce ringing artifacts [113]. Malfait *et al.* proposed a stochastic extension of this approach using Markov random field models [58].

2) *Image Enhancement*: The task here is to accentuate image features that are clinically relevant and that may be difficult to visualize under normal viewing conditions (e.g., X-ray film on a light box). Image enhancement is especially relevant in mammography where the contrast between the soft tissues of the breast is inherently small, and a relatively minor change in mammary structure can signify the presence of a malignant breast tumor. Because of the current emphasis on mammographic screening, wavelet-based enhancement methods have been primarily designed with that application in mind [50], [81], [49]. These approaches all use a reversible wavelet decomposition, which may be redundant or not, and perform the enhancement by selective modification (amplification) of certain wavelet coefficients prior to reconstruction. Laine *et al.* used a point nonlinearity that is either global (histogram modification) or local and controlled by the edges at the corresponding resolution [50], [49]. Note that when the weighting scheme is linear, this approach can be interpreted as a multiscale version of traditional unsharp masking [48]. The improvement in performance over the standard enhancement techniques reported by Laine *et al.* supports the notion that wavelets are useful for improving the detectability of important mammographic features [49], [112]. A possible extension, which is briefly described in [78], is to replace the point nonlinearity in the wavelet domain by a nonlinear adaptive filter. Contrast enhancement can also be performed in the context of Mallat and Zhong's algorithm by accentuating selected maxima in the multiscale edge representation of the image [55]. Note that these enhancement techniques are not fundamentally different from the noise reduction methods described previously. In one case, one amplifies certain signal features of interest, while in the other, one suppresses the unwanted noise components.

3) *Detection of Microcalcifications in Mammograms*: One of the key issues in computer-assisted mammography is the detection of clusters of fine, granular microcalcifications, which constitute one of the primary warning signs of breast cancer. Individual grains (μ CA++) typically range in size from 0.05–1 mm in diameter. The detection of μ CA++s is closely related to the previous enhancement task and the methods developed are very similar, except that the detection is typically performed by thresholding (or classification) in the wavelet domain [19], [79], [92], [116]. Clarke *et al.* found some advantages in using specifically designed three channel quadrature mirror filterbanks instead of the

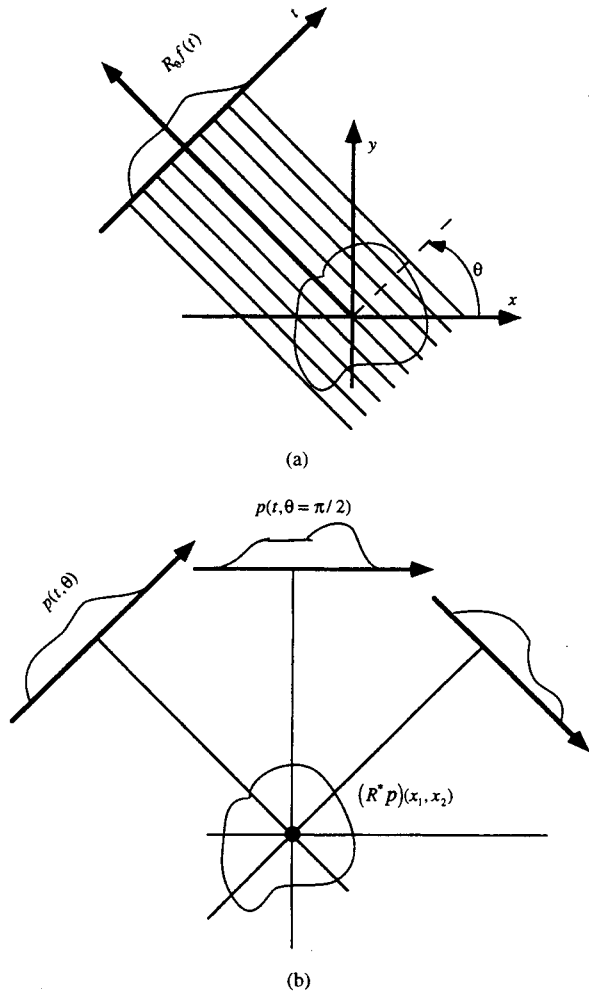


Fig. 4. Basic tomographic operators. (a) The tomographic projection $R_\theta f(t)$ is the collection of parallel ray integrals through the object f in the direction specified by θ ; the Radon transform is the set of all such angular projections for $\theta \in [0, \pi]$. (b) The backprojection operator provides a reverse mapping from the Radon domain back to the object domain. Specifically, $(R^* p)(\mathbf{x})$ represents the angular average of all projection contributions $p(t, \theta)$ originating for the point \mathbf{x} .

more conventional two channel solution [19]. Strickland used an overcomplete WT detector, which he showed to be closely related to the prewhitening matched filter for the detection of Gaussian objects (idealized microcalcifications) in Markov noise (background noise) [92] (Section II-C). Barman *et al.* based their detection on a more complete object description using local shape parameters derived from a wavelet-like multiscale decomposition that uses directional quadrature filters [11]. The detection results reported so far suggest that these new wavelet techniques perform better than the best available single-scale methods [19], [92], [116].

B. Computer-Assisted Tomography (CAT)

The problem of 2-D computerized X-ray tomography is to reconstruct an object $f(\mathbf{x})$, $\mathbf{x} = (x_1, x_2) \in \mathbb{R}^2$ from the measured values of its angular projections. These measurements are described by the Radon transform of f which provides the line-integrals of f along the direction

specified by the angle θ [Fig. 4(a)]

$$R_\theta f(t) = \int_{-\infty}^{+\infty} f(t \cos \theta - u \sin \theta, t \sin \theta + u \cos \theta) du. \quad (8)$$

In the idealized case in which the variables \mathbf{x} , t , and θ are continuously defined, the inversion formula is provided by the well-known filtered-backprojection (FBP) identity [80], [57]

$$f = R^* K R_\theta f = R^*(q * R_\theta f) \quad (9)$$

which is valid for any function in $L_2(\mathbb{R}^2)$. The operator K in (9) represents the filtering part of the formula, in which each projection is convolved with the ramp filter q whose Fourier transform is

$$\hat{q}(\omega) = |\omega|. \quad (10)$$

The adjoint operator R^* is the backprojection

$$(R^* p)(\mathbf{x}) = \frac{1}{\pi} \int_0^\pi p(x_1 \cos \theta + x_2 \sin \theta, \theta) d\theta \quad (11)$$

which computes the angular average of all projection contributions originating for the point \mathbf{x} ; i.e., the (filtered) projection values $p(t, \theta) = (q * R_\theta f)(t)$ with $t = x_1 \cos \theta + x_2 \sin \theta$ and $\theta \in [0, \pi]$ (Fig. 4(b)). Note that the continuous FBP formula (9) is equivalent to the central slice theorem which states that the 1-D Fourier transform of $R_\theta f(t)$ is a line through the 2-D Fourier transform of f .

The primary motivation for using wavelets for tomography is that the spatial delocalization effect of the ramp filter $\hat{q}(\omega)$, which is due to its singularity at $\omega = 0$, is greatly attenuated by the corresponding zeros of the wavelet functions (vanishing moments) [70]. Hence, wavelet reconstruction formulas tend to be localized spatially and can be applied to obtain partial reconstructions when only a portion of the Radon transform is available (limited-angle tomography) [15].

The simplest approach to obtain a wavelet reconstruction of f is to evaluate the 2-D wavelet coefficients of f directly using (9). For this purpose, we first convolve f with the rescaled 2-D analysis function $\varphi_a(\mathbf{x}) = a^{-1/2} \varphi(\mathbf{x}/a)$ and rewrite the FBP identity for this prefiltered signal

$$\begin{aligned} \varphi_a * f &= R^* K R_\theta (\varphi_a * f) = R^* K (R_\theta \varphi_a * R_\theta f) \\ &= R^*(q_{a,\theta} * R_\theta f) \end{aligned} \quad (12)$$

where, on the right-hand side, we have combined the Radon transform of the 2-D analysis function with q into a modified (angle-dependent) ramp filter

$$q_{a,\theta}(t) = (q * R_\theta \varphi_a)(t). \quad (13)$$

Note that in the wavelet case, this filter tends to be much better localized than q in (10). We can then compute the desired 2-D inner products (wavelet or spline coefficients) by using modified resampled FBP scheme

$$\begin{aligned} c_a(\mathbf{k}) &= a^{-1/2} \langle f(\mathbf{x}), \varphi(\mathbf{x}/a - \mathbf{k}) \rangle \\ &= R^*(q_{a,\theta} * R_\theta f)(\mathbf{x})|_{\mathbf{x}=\mathbf{k}/a}. \end{aligned} \quad (14)$$

which only requires the computation of the backprojection on the lattice at the corresponding scale. This approach was first proposed for fixed-scale tomographic reconstruction using splines [36]–[38]. The scheme is directly applicable for the reconstruction of the wavelet coefficients of the function and has been investigated by several authors [37], [47], [27].

An alternative approach promoted by Olson *et al.* is to start by decomposing the Radon transforms in terms of a wavelet basis [70]. The advantage of this procedure is that one can make use of the range properties of the Radon transform to interpolate for missing angles. In particular, Olson showed that the Radon wavelet coefficients as a function of θ are essentially bandlimited with a bandwidth inversely proportional to their scale.

Another interesting observation is that if the analysis function $\varphi = \psi$ is a circularly symmetric wavelet with sufficient decay in frequency, then the modified ramp filter is an admissible wavelet as well, so that we can interpret (12) as a relation that links the CWT of f to the CWT of its Radon transform [75], [76], [105].

Finally, the WT also appears to have some merit for noise reduction in tomography. Two approaches that have been considered are wavelet shrinkage [47], and a wavelet-constrained version of linear least squares estimation [86].

C. Magnetic Resonance Imaging (MRI)

When exposed to a large external static magnetic field, the nuclear spins in a specimen tend to resonate and precess at the Larmor frequency $f_{\text{Lamor}} = \gamma H_0$, which is proportional to the external field H_0 . MRI exploits this phenomenon and produces images through spatially selective excitation. The spatial encoding is achieved by applying suitable gradient fields in the three principal directions (x, y, z) . During a measurement sequence, the spins in a selected portion of the specimen (e.g., a slice) are excited by the application of a radio frequency (RF) pulse. The precessing magnetizations in the transverse plane generate a small oscillating voltage in the pickup coil, a signal that dies out progressively as the spins lose their energy and realign with the external field. Thus the Fourier transform of the received signal can be used to determine the density of the spins resonating at the various frequencies. The resonance frequency is typically modified linearly along the x -axis (or any other direction) by switching on the corresponding gradient field during the measurement (frequency encoding). An additional subtlety is that the readout is not performed on the primary signal but on an echoed version of it which eliminates most sources of dephasing not directly related to the specimen (field inhomogeneities, etc.). Spin echoing is induced by applying a second 180° RF pulse reversing the phases of the spins in the sample. Conventional spin-echo imaging requires N repeated measurements of this type and uses frequency encoding in the x -direction and phase encoding in the y -direction. The additional phase shift is introduced by submitting the sample to a y -gradient of appropriate strength during a certain time interval T_p prior to recording. The image is then reconstructed by 2-D inverse Fourier transformation.

The idea behind wavelet encoding, as proposed by Weaver and Healy [111], [39], is that one can shape the RF excitation and select a 2-D portion of the specimen as if it was viewed through a weighting function. In this setup, the MR signal collected at the center of the echo is modeled by the following inner product

$$c_k(t) = \iint \rho(x, y) \varphi_k(y) e^{jG_x x t} dx dy \quad (15)$$

where $\rho(x, y)$ is the effective 2-D spin density in the slice of interest, $\varphi_k(y)$ the analysis function (or excitation profile) in the y -direction, and $e^{jG_x x t}$ the frequency encoding term in the x -direction introduced by the readout gradient. Such a selective excitation is obtained by applying an RF pulse that corresponds to the inverse Fourier transform of $\varphi_k(y)$. An example of implementation is shown in Fig. 5. Thus if we acquire N such measurements against a set of basis functions $\{\varphi_k(y)\}_{k=1, \dots, N}$, we can reconstruct the spin density function $\rho(x, y)$ by appropriate 2-D inverse transformation (Fourier in the t -dimension and φ -based along k).

Conventional phase-encoded MRI uses Fourier basis functions³ that are completely delocalized spatially. As a result, the method is relatively slow because of the need to wait for all the spins in the specimen to realign before a new measurement can be made. Wavelet bases, on the other hand, are much better localized spatially and offer the possibility of a faster repetition rate [111], [39]. The practical feasibility of the wavelet approach was demonstrated by Panich *et al.* who imaged 2-D samples using Battle–Lemarié spline wavelets [73]. Currently, it appears that the main advantages of wavelet-encoded MRI are the possibility of faster acquisition with the ability to generate T2 weighted spin echo images one slice at the time, and the reduction of motion artifacts. However, speed in MRI always comes at the expense of signal-to-noise ratio. It is still possible to trade one property for the other by using more general wavelet-packets basis functions [109]. Likewise, one can attempt to obtain the best quality reconstruction with the smallest number of measurements by using Karhunen–Loève type basis functions [40].

The multiresolution properties of the WT can also be used advantageously for fast image sequence acquisition. Olson *et al.* proposed a tomographic MRI acquisition scheme in which the information at different scales is updated at different rates [72]; in particular, low frequency components can be reconstructed almost instantaneously and used to estimate the motion of the object which is then used to compensate for the displacement of the fine structures [71]. Panich *et al.* described a similar dynamic acquisition scheme that adaptively locates and then finely resolves only those regions of the field of view where change is occurring [74].

As far as speed is concerned, these wavelet methods are still not competitive with the more recent echo-planar imaging techniques that can acquire an entire slice in a single echo. However, the use of echo planar MRI is currently limited because of the costly hardware that is required (very

³Specifically, $\varphi_k(y) = e^{jkT_p G_0 y}$, where kG_0 is the strength of the y -gradient at the k th measurement.

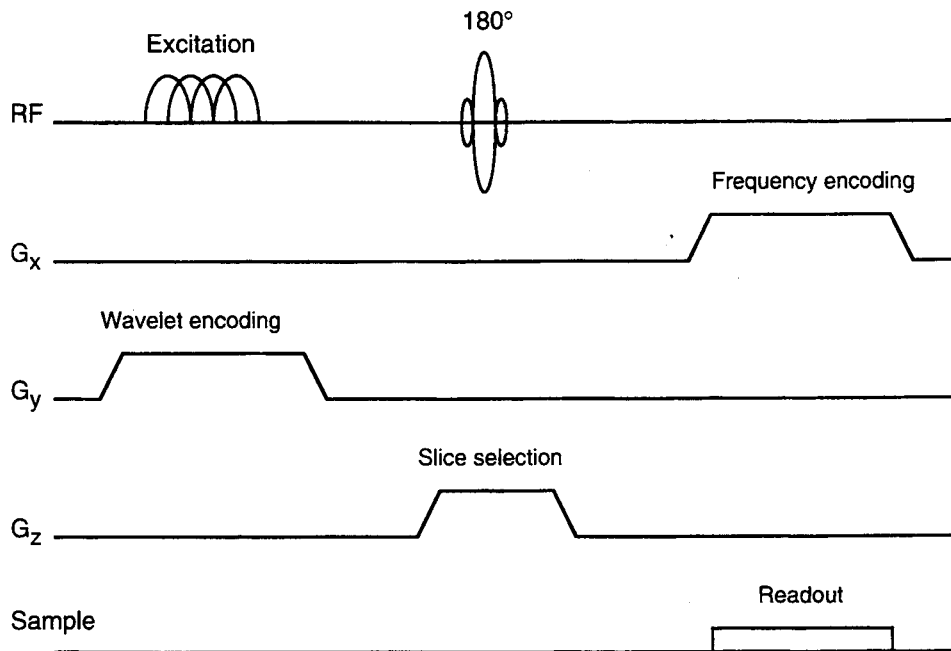


Fig. 5. Simplified representation of the pulse sequence used by Panich *et al.* for single section wavelet-encoded MRI. The sequence of events is as follows: 1) The sample is excited using a small flip angle wavelet-shaped RF pulse which is applied in conjunction with a linear gradient (G_y); this achieves a selective excitation in the y -direction. 2) The slice of interest is selected through the application of a spatially selective (z -axis) sinc-shaped 180° pulse. 3) Finally, the MR signal is measured with the x -gradient turned on; this achieves the frequency encoding in the x -direction.

large, very fast, switched gradients). It is also more prone to artifacts and has a much lower signal-to-noise ratio.

D. Functional Image Analysis (PET and fMRI)

Functional neuroimaging is a fast developing area aimed at investigating the neuronal activity of the brain *in vivo*. The data for those studies is provided by PET and fMRI. PET measures the spatial distribution of certain function-specific radiotracers injected into the bloodstream prior to imaging. A typical example is the measurement of cerebral glucose utilization with the tracer $[^{18}\text{F}]2$ -fluoro-2-deoxy-D-glucose (FDG). fMRI, which is a more recent technique, allows for a visualization of local changes in blood oxygenation believed to be induced by neuronal activation. It is substantially faster than PET and also offers better spatial resolution. Yet there is still disagreement among specialists concerning the exact nature of the biological processes that produce the observed changes in the MR signal.

The functional images obtained with those two modalities are extremely noisy and variable, and their interpretation requires the use of statistical analysis methods [103]. What is typically of interest is the detection of the differences of activity between different groups of subjects (e.g., normal versus diseased) or between different experimental conditions with the same subject (e.g., rest versus word generation). In either case, the variability of the signal is such that multiple subjects or repeated trials are required in each subgroup.

The first step in this analysis is to register the various images so that they can be compared on a pixel-by-pixel

basis. The registration can be used to compensate for inter-subject anatomical variability (which is acceptable for low resolution PET data), or for intrasubject movement in the scanner. Efficient multiresolution solutions to this problem have been proposed first in 2-D for rigid body motion (rotation and translation) [101], and more recently in 2-D-3-D using the more general affine transformation model [94], [95]. In both cases, the images or volumes are represented by a spline multiresolution and the registration parameters are determined iteratively using a coarse-to-fine refinement strategy. As a result, the algorithm is much faster and more robust than a comparable single-scale implementation. So far, the method has been successfully applied to inter-subject PET registration using the general affine model, and intrasubject (rigid body) registration in fMRI [95].

The second step is to compute the difference between the aligned group averages and perform the statistical analysis. Testing in the image domain directly is difficult because of the amount of residual noise and the necessity to use a very conservative significance level to compensate for multiple testing (one test per pixel!). A better solution is to perform the testing in the wavelet domain [85], [82], [103]. The main advantage is that the discriminative information, which is smooth and well localized spatially, becomes concentrated into a relatively small number of coefficients, while the noise remains evenly divided among all coefficients. In addition, the number of statistical tests can be reduced considerably by first identifying the few wavelet channels that contain significant differences. A

recent application of this technique to fMRI is presented in [84].

V. CONCLUSION

As this review shows, the uses of the WT in biomedical applications are extremely diverse. All the recent successes that have been obtained in this area should be attributed to the versatility of the wavelet tools, especially with respect to their localization properties in the time-frequency (or space-frequency) plane. The principle of a multiscale analysis also appears to be justified whenever the initial sampling rate of the signal is not necessarily adapted to the phenomena that are of interest to the investigator. It is also satisfying to note the analogy between these mathematical tools and certain forms of low level processing that occur in the auditory and visual system.

However, wavelets are not a panacea and they should be used with caution. The selection of a particular solution should always be motivated by the problem itself and our understanding of the underlying biology and physics, rather than by the tools that are currently available and fashionable. As more and more wavelet solutions are proposed, these methods will only be credible if they are shown to outperform the best techniques otherwise available. Thus comparative studies are needed more than ever.

REFERENCES

- [1] M. Akay, Y. M. Akay, P. Cheng, and H. H. Szeto, "Time-frequency analysis of the electrocortical activity during maturation using wavelet transform," *Biol. Cybern.*, vol. 71, no. 2, pp. 169-176, 1994.
- [2] M. Akay, Y. M. Akay, W. Welkowitz, and S. Lewkowicz, "Investigating the effects of vasodilator drugs on the turbulent sound caused by femoral artery stenosis using short-term Fourier and wavelet transform methods," *IEEE Trans. Biomed. Eng.*, vol. 41, pp. 921-928, Oct. 1994.
- [3] M. Akay *et al.*, "Carotid-cardiac interaction: heart rate variability during the unblocking of the carotid artery," *Adv. Exp. Med. Biol.*, vol. 346, no. 72, pp. 365-372, 1993.
- [4] M. Akay and H. H. Szeto, "Wavelet analysis of opioid drug effects on the electrocortical activity in fetus," in *Proc. Conf. Artif. Neural Networks in Eng.*, 1994, pp. 553-558.
- [5] Y. M. Akay, M. Akay, W. Welkowitz, and J. Kostis, "Noninvasive detection of coronary artery disease," *IEEE Eng. in Med. and Biol. Mag.*, vol. 13, no. 5, pp. 761-764, 1994.
- [6] S. Akselrod *et al.*, "Power spectrum analysis of heart rate fluctuation: a quantitative probe of beat-to-beat cardiovascular control," *Sci.*, vol. 213, pp. 220-223, 1981.
- [7] A. Aldroubi and M. Unser, Eds., *Wavelets in Medicine and Biology*. Boca Raton, FL: CRC, 1996.
- [8] ———, "Families of multiresolution and wavelet spaces with optimal properties," *Numerical Functional Analysis and Optimiz.*, vol. 14, no. 5-6, pp. 417-446, 1993.
- [9] P. A. Angelidis, "MR image compression using a wavelet transform coding algorithm," *Magn. Reson. Imaging*, vol. 12, no. 7, pp. 1111-20, 1994.
- [10] M. Antonini, M. Barlaud, P. Mathieu, and I. Daubechies, "Image coding using wavelet transform," *IEEE Trans. Image Process.*, vol. 1, pp. 205-220, Feb. 1992.
- [11] H. Barman, G. Granlund, and L. Haglund, "Feature extraction for computer-aided analysis of mammograms," *Int. J. Patt. Recog. and Artif. Intell.*, vol. 7, no. 6, pp. 1339-1356, 1993.
- [12] E. A. Bartnik, K. J. Blinowska, and P. J. Durka, "Single evoked potential reconstruction by means of wavelet transform," *Biolog. Cybern.*, vol. 67, no. 2, pp. 175-181, 1992.
- [13] A. Baskurt, F. Peyrin, H. Benoit-Cattin, and R. Goutte, "Coding of 3D medical images using 3D wavelet decompositions: Wavelet-based tool for medical image compression," in *Proc. IEEE Int. Conf. on Acoust., Speech and Signal Process.*, Minneapolis, MN, Apr. 1993, vol. 5, pp. 562-565.
- [14] J. J. Benedetto and A. Teolis, "A wavelet auditory model and data compression," *Appl. Computat. Harmonic Anal.*, vol. 1, pp. 3-28, 1993.
- [15] C. Berenstein and D. Walnut, "Local inversion of the Radon transform in even dimensions using wavelets," in *75 Years of Radon Transform*, S. Gindikin and P. Michor, Eds. Cambridge, MA: International Press, 1994, pp. 45-69.
- [16] O. Bertrand, J. Bohorquez, and J. Pernier, "Time-frequency digital filtering based on an invertible wavelet transform: an application to evoked potentials," *IEEE Trans. Biomed. Eng.*, vol. 41, pp. 77-88, Jan. 1994.
- [17] K. J. Blinowska and P. J. Durka, "Application of wavelet transform and matching pursuit to the time-varying EEG signals," in *Proc. Conf. Artif. Neural Networks in Eng.*, 1994, pp. 535-540.
- [18] R. Carmona and L. Hudgins, "Wavelet de-noising of EEG signals and identification of evoked response potentials," in *Proc. SPIE Conf. Wavelet Applicat. in Signal and Image Process. II*, San Diego, CA, July 1994, vol. 2303, pp. 91-104.
- [19] L. P. Clarke *et al.*, "Tree-structured nonlinear filter and wavelet transform for microcalcification segmentation in digital mammography," *Cancer Lett.*, vol. 77, no. 2-3, pp. 173-81, 1994.
- [20] A. Cohen and J. Kovacevic, "Wavelets: the mathematical background," *Proc. IEEE*, this issue, pp. 514-522.
- [21] I. Daubechies, "Orthogonal bases of compactly supported wavelets," *Comm. Pure Appl. Math.*, vol. 41, pp. 909-996, 1988.
- [22] ———, *Ten Lectures on Wavelets*. Philadelphia, PA: Soc. Ind. and Appl. Math., 1992.
- [23] J. G. Daugman, "Complete discrete 2-D Gabor transforms by neural networks for image analysis and compression," *IEEE Trans. Acoust., Speech and Signal Process.*, vol. 36, pp. 1169-1179, July 1988.
- [24] ———, "Entropy reduction and decorrelation in visual coding by oriented neural receptive fields," *IEEE Trans. Biomed. Eng.*, vol. 36, pp. 107-114, Jan. 1989.
- [25] R. De Valois and K. De Valois, *Spatial Vision*. New York: Oxford Univ. Press, 1988.
- [26] R. L. De Valois, D. G. Albrecht, and L. G. Thorell, "Cortical cells: bar and edge detectors, or spatial frequency filters," in *Frontiers in Visual Science*, S. J. Cool and E. L. Smith III, Eds. New York: Springer, 1978, pp. 544-556.
- [27] A. H. Delaney and Y. Bresler, "Multiresolution tomographic reconstruction using wavelets," *IEEE Trans. Image Process.*, vol. 6, pp. 799-813, June 1995.
- [28] R. A. DeVore, B. Jawerth, and B. J. Lucier, "Image compression through wavelet transform coding," *IEEE Trans. Inform. Theory*, vol. 38, pp. 719-746, Feb. 1992.
- [29] R. A. DeVore and B. J. Lucier, "Fast wavelet techniques for near-optimal image processing," in *Proc. IEEE Military Commun. Conf.*, New York, 1992, pp. 48.3.1-48.3.7.
- [30] H. Dickhaus, L. Khadra, and J. Brachmann, "Time-frequency analysis of ventricular late potentials," *Methods of Inform. in Med.*, vol. 33, no. 2, pp. 187-195, 1994.
- [31] D. L. Donoho, "De-noising by soft-thresholding," *IEEE Trans. Inform. Theory*, vol. 41, pp. 613-627, Mar. 1995.
- [32] D. L. Donoho and I.M. Johnstone, "Ideal spatial adaptation via wavelet shrinkage," *Biometrika*, vol. 81, pp. 425-455, 1994.
- [33] ———, "Threshold selection for wavelet shrinkage of noisy data," in *Proc. IEEE EMBS Workshop on Wavelets in Med. and Biol.*, Baltimore, 1994, pp. 24a-24b.
- [34] L. Gaudart, J. Crebassa, and J. P. Petrakian, "Wavelet transform in human visual channels," *Applied Optics*, vol. 32, no. 22, pp. 4119-4127, 1993.
- [35] M. H. Goldstein, Jr., "Auditory periphery as speech signal processor," *IEEE Eng. in Med. and Biol. Mag.*, vol. 13, no. 2, pp. 186-196, 1994.
- [36] J.-P. Guedon and Y. Bizais, "Bandlimited and Haar filtered backprojection reconstructions," *IEEE Trans. Med. Imag.*, vol. 13, pp. 430-440, Mar. 1994.
- [37] J.-P. Guédon and M. Unser, "Least squares and spline filtered back-projection," NCCR Rep. 52/92, Nat. Inst. Health, 1992.
- [38] J.-P. Guedon, M. Unser, and Y. Bizais, "Pixel intensity distribution models for filtered back-projection," in *Proc. IEEE Med. Imaging Conf.*, Santa Fe, NM, 1991, vol. 3, pp. 2063-2067.
- [39] D. M. Healy, Jr. and J. B. Weaver, "Two applications of wavelet transforms in magnetic resonance," *IEEE Trans. Inform. Theory*, vol. 38, pp. 840-860, 1992.
- [40] ———, "Joint best bases for fast encoding in magnetic resonance

- imaging," in *Proc. Int. Conf. on Acoust., Speech and Signal Process.*, Detroit, MI, 1995, vol. 5, pp. 2923–2926.
- [41] C. Heneghan *et al.*, "Investigating the nonlinear dynamics of cellular motion in the inner ear using the short-time Fourier and continuous wavelet transforms," *IEEE Trans. Signal Process.*, vol. 42, pp. 3335–3352, Dec. 1994.
- [42] D. H. Hubel, "Exploration of the primary visual cortex: 1955–1978," *Nature*, vol. 299, pp. 515–524, 1982.
- [43] T. Kalayci and O. Ozdamar, "Wavelet preprocessing for automated neural-network detection of spikes," *IEEE Eng. in Med. and Biol. Mag.*, vol. 14, no. 2, pp. 160–166, 1995.
- [44] M. Karrakchou, C. V. Lambrecht, and M. Kunt, "Analyzing pulmonary capillary-pressure—more accurate measurements using mutual wavelet packets for adaptive filtering," *IEEE Eng. in Med. and Biol. Mag.*, vol. 14, no. 2, pp. 179–185, 1995.
- [45] L. Khadra, H. Dickhaus, and A. Lipp, "Representations of ECG-late potentials in the time frequency plane," *J. Med. Eng. and Technol.*, vol. 17, no. 6, pp. 228–231, 1993.
- [46] L. Khadra, M. Matalgah, B. El-Asir, and S. Mawagdeh, "The wavelet transform and its applications to phonocardiogram signal analysis," *Med. Informat.*, vol. 16, no. 3, pp. 271–277, 1991.
- [47] E. D. Kolaczyk, "Wavelet shrinkage in tomography," in *Proc. IEEE EMBS Workshop on Wavelets in Med. and Biol.*, Baltimore, 1994, pp. 1206–1207.
- [48] A. Laine, J. Fan, and S. Schuler, "On discrete dyadic wavelets for contrast enhancement," in *Proc. SPIE Conf. Wavelet Applicat. in Signal and Image Process. II*, San Diego, CA, July 1994, vol. 2303, pp. 456–460.
- [49] A. F. Laine, S. Schuler, F. Jian, and W. Huda, "Mammographic feature enhancement by multiscale analysis," *IEEE Trans. Med. Imag.*, vol. 13, pp. 725–740, Apr. 1994.
- [50] A. F. Laine and S. Song, "Multiscale wavelet representations for mammographic feature analysis," in *Proc. SPIE Conf. Mathemat. Methods in Med. Imag.*, 1992, vol. 1768, pp. 306–316.
- [51] A. S. Lewis and G. Knowles, "Image compression using the 2-D wavelet transform," *IEEE Trans. Image Process.*, vol. 1, pp. 244–250, Feb. 1992.
- [52] C. Li and C. Zheng, "QRS detection by wavelet transform," in *Proc. Annu. Conf. on Eng. in Med. and Biol.*, 1993, vol. 15, pp. 330–331.
- [53] C. Li, C. Zheng, and C. Tai, "Detection of ECG characteristic points using wavelet transforms," *IEEE Trans. Biomed. Eng.*, vol. 42, no. 1, pp. 21–28, 1995.
- [54] L. M. Lim, M. Akay, and J. A. Daubenspeck, "Identifying respiratory-related evoked potentials," *IEEE Eng. in Med. and Biol. Mag.*, vol. 13, no. 2, pp. 174–178, 1995.
- [55] J. Lu, D. M. Healy, Jr. and J. B. Weaver, "Contrast enhancement of medical images using multiscale edge representation," *Opt. Eng.*, vol. 33, no. 7, pp. 2151–2161, 1994.
- [56] B. J. Lucier *et al.*, "Wavelet compression and segmentation of digital mammograms," *J. Digit. Imag.*, vol. 7, no. 1, pp. 27–38, 1994.
- [57] D. Ludwig, "The radon transform on Euclidean space," *Comm. on Pure and Appl. Mathematics*, vol. 19, pp. 49–81, 1966.
- [58] M. Malfait and D. Roose, "Biomedical Image Denoising with wavelets and Bayesian geometrical constraints," in *Proc. IEEE EMBS Workshop on Wavelets in Med. and Biol.*, Baltimore, 1994, vol. 2, pp. 1228–1229.
- [59] S. Mallat and W. L. Hwang, "Singularity detection and processing with wavelets," *IEEE Trans. Informat. Theory*, vol. 38, pp. 617–643, Feb. 1992.
- [60] S. Mallat and S. Zhong, "Characterization of signals from multiscale edges," *IEEE Trans. Patt. Anal. Machine Intell.*, vol. 14, pp. 710–732, July 1992.
- [61] S. G. Mallat, "Multifrequency channel decompositions of images and wavelet models," *IEEE Trans. Acoust., Speech and Signal Process.*, vol. 37, pp. 2091–2110, Dec. 1989.
- [62] ———, "Multiresolution approximations and wavelet orthogonal bases of $L^2(\mathbb{R})$," *Trans. Amer. Math. Soc.*, vol. 315, no. 1, pp. 69–87, 1989.
- [63] ———, "A theory of multiresolution signal decomposition: the wavelet representation," *IEEE Trans. Patt. Anal. Mach. Intell.*, vol. 11, pp. 674–693, July 1989.
- [64] A. Manduca, "Wavelet-based tool for medical image compression," in *Proc. SPIE Conf. Medical Imaging VI: Image Capture, Formatting, and Display*, 1992, vol. 1653, pp. 495–503.
- [65] ———, "Medical image compression with wavelet/subband coding," in *Proc. Conf. Artif. Neural Networks in Eng.*, 1994, pp. 645–650.
- [66] E. Mannheimer, "Kalibrierte Phonokardiographie," *Cardiologia*, vol. 6, pp. 281–302, 1942.
- [67] S. Marcelja, "Mathematical description of the responses of simple cortical cells," *J. Opt. Soc. Amer.*, vol. 70, no. 11, pp. 1297–1300, 1980.
- [68] O. Meste, H. Rix, P. Caminal, and N. V. Thakor, "Ventricular late potentials characterization in time-frequency domain by means of a wavelet transform," *IEEE Trans. Biomed. Eng.*, vol. 41, pp. 625–634, July 1994.
- [69] M. S. Obaidat, "Phonocardiogram signal analysis: techniques and performance," *J. Med. Eng. and Technol.*, vol. 17, pp. 221–227, 1993.
- [70] T. Olson and J. DeStefano, "Wavelet localization of the Radon transform," *IEEE Trans. Signal Process.*, vol. 42, pp. 2055–2067, Aug. 1994.
- [71] T. Olson, D. Healy, and J. Weaver, "Reduced motion artifacts in magnetic resonance imaging by adaptive spatio-temporal multiresolution reconstruction," in *Proc. SPIE Conf. Wavelet Applicat. in Signal and Image Process. II*, San Diego, CA, July 1994, vol. 2303, pp. 442–455.
- [72] T. Olson, D. Healy, J. B. Weaver, and J. S. DeStefano, "Fast updating in MRI via multiscale localization," in *Proc. SPIE Conf. Wavelet Applicat. in Signal and Image Process.*, San Diego, CA, 1993, vol. 2034, pp. 70–83.
- [73] L. P. Panych, P. D. Jakab, and F. A. Jolesz, "Implementation of wavelet-encoded MR imaging," *J. Magn. Reson. Imaging*, vol. 3, no. 4, pp. 649–655, 1993.
- [74] L. P. Panych and F. A. Jolesz, "A dynamically adaptive imaging algorithm for wavelet-encoded MRI," *Magn. Reson. Med.*, vol. 32, pp. 738–748, 1994.
- [75] F. Peyrin, M. Zaim, and R. Goutte, "Multiscale reconstruction of tomographic images," in *Proc. IEEE-SP Int. Symp. Time-Frequency and Time-Scale Analysis*, Victoria, BC, Canada, Oct. 1992, pp. 219–222.
- [76] F. Peyrin, M. Zaim, and R. Goutte, "Construction of wavelet decompositions for tomographic images," *J. Mathemat. Imag. and Vision*, vol. 3, no. 1, pp. 105–121, 1993.
- [77] M. Porat and Y. Y. Zeevi, "Localized texture processing in vision: analysis and synthesis in Gaborian space," *IEEE Trans. Biomed. Eng.*, vol. 36, pp. 115–129, Jan. 1989.
- [78] W. Qian *et al.*, "Application of wavelet transform for image enhancement in medical imaging," in *Proc. Conf. Artif. Neural Networks in Eng.*, 1994, pp. 651–660.
- [79] W. Qian *et al.*, "Digital mammography: m -channel quadrature mirror filters (QMF's) for microcalcification extraction," *Computerized Med. Imaging and Graphics*, vol. 18, no. 5, pp. 301–314, 1994.
- [80] J. Radon, "Über die Bestimmung von Functionen durch ihre Integralwerte langs gewisser Mannigfaltigkeiten," *Math.-Phys. Kl.*, vol. 69, pp. 262–267, 1917.
- [81] W. B. Richardson, Jr., "Nonlinear filtering and multiscale texture discrimination for mammograms," in *Proc. SPIE Conf. Mathemat. Methods in Med. Imag.*, 1992, vol. 1768, pp. 293–305.
- [82] D. E. Rio, R. R. Rawlings, U. E. Ruttimann, and R. Momenan, "Study of statistical methods applied in the spatial, wavelet and Fourier domain to enhance and analyze group characteristics of images: application to positron emission tomography brain images," in *Proc. SPIE Conf. Mathemat. Methods in Med. Imag. III*, 1994, vol. 2299, pp. 194–206.
- [83] O. Rioul and P. Duhamel, "Fast algorithms for discrete and continuous wavelet transforms," *IEEE Trans. Inform. Theory*, vol. 38, pp. 569–586, Feb. 1992.
- [84] U. E. Ruttimann *et al.*, "Analysis of functional magnetic resonance images by wavelet decomposition," in *Proc. Int. Conf. on Image Process.*, Washington, DC, 1995, vol. 1, pp. 633–636.
- [85] U. E. Ruttimann, M. Unser, D. Rio, and R. R. Rawlings, "Use of the wavelet transform to investigate differences in brain PET images between patients," in *Proc. SPIE Conf. Mathemat. Methods in Med. Imaging II*, San Diego, CA, July 1993, vol. 2035, pp. 192–203.
- [86] B. Sahiner and A. E. Yagle, "Image reconstruction from projections under wavelet constraints," *IEEE Trans. Signal Process.*, vol. 41, pp. 3579–3584, Dec. 1993.
- [87] R. Sartene *et al.*, "Using wavelet transform to analyze cardiorespiratory and electroencephalographic signals during sleep," in

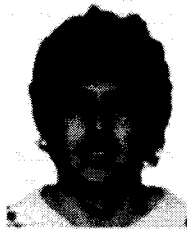
- Proc. IEEE EMBS Workshop on Wavelets in Med. and Biol.*, Baltimore, 1994, pp. 18a-19a.
- [88] S. J. Schiff, A. Aldroubi, M. Unser, and S. Sato, "Fast wavelet transformation of EEG," *Electroencephalogr. Clin. Neurophysiol.*, vol. 91, no. 6, pp. 442-455, 1994.
- [89] S. J. Schiff, J. Milton, J. Heller, and S. L. Weinstein, "Wavelet transforms and surrogate data for electroencephalographic and seizure localization," *Opt. Eng.*, vol. 33, no. 7, pp. 2162-2169, 1994.
- [90] L. Senhadji, G. Carrault, J. J. Bellanger, and G. Passariello, "Comparing wavelet transforms for recognizing cardiac patterns," *IEEE Eng. in Med. and Biol. Mag.*, vol. 14, no. 2, pp. 167-173, 1995.
- [91] J. M. Shapiro, "Embedded image coding using zerotrees of wavelet coefficients," *IEEE Trans. Signal Process.*, vol. 41, pp. 3445-3462, Dec. 1993.
- [92] R. N. Strickland and H. I. Hahn, "Detection of microcalcifications in mammograms using wavelets," in *Proc. SPIE Conf. Wavelet Applicat. in Signal and Image Process. II*, San Diego, CA, July 1994, vol. 2303, pp. 430-441.
- [93] N. V. Thakor, X.-R. Guo, Y.-C. Sun, and D. F. Hanley, "Multiresolution wavelet analysis of evoked potentials," *IEEE Trans. Biomed. Eng.*, vol. 40, pp. 1085-1094, Nov. 1993.
- [94] P. Thévenaz and M. Unser, "Efficient geometric transformations and 3-D image registration," in *Proc. Int. Conf. on Acoust., Speech and Signal Process.*, Detroit, MI, May 1995, vol. 5, pp. 2919-2923.
- [95] —, "Iterative multi-scale image registration without landmarks," in *Proc. Int. Conf. on Image Process.*, Washington, DC, 1995, vol. 3, pp. 228-231.
- [96] H. Tsuji and H. Mori, "New analysis of HRV through wavelet transform," *Int. J. Human-Computer Interaction*, vol. 6, no. 2, pp. 205-217, 1994.
- [97] F. Tuteur, "Wavelet transformations in signal detection," in *Wavelets: Time-Frequency Methods and Phase Space*, J. Combes, A. Grossman, and P. Tchamitchian, Eds. New York: Springer-Verlag, 1989, pp. 132-137.
- [98] M. Unser, "Fast Gabor-like windowed Fourier and continuous wavelet transforms," *IEEE Signal Process. Lett.*, vol. 1, pp. 76-79, May 1994.
- [99] —, "Texture classification and segmentation using wavelet frames," *IEEE Trans. Image Process.*, vol. 4, pp. 1549-1560, Nov. 1995.
- [100] M. Unser, A. Aldroubi, and M. Eden, "On the asymptotic convergence of B-spline wavelets to Gabor functions," *IEEE Trans. Informat. Theory*, vol. 38, pp. 864-872, Feb. 1992.
- [101] M. Unser, A. Aldroubi, and C. R. Gerfen, "A multiresolution image registration procedure using spline pyramids," in *Proc. SPIE Conf. Wavelet Applicat. in Signal and Image Process.*, San Diego, CA, 1993, vol. 2034, pp. 160-170.
- [102] M. Unser, A. Aldroubi, and S. J. Schiff, "Fast implementation of the continuous wavelet transform with integer scales," *IEEE Trans. Signal Process.*, vol. 42, pp. 3519-3523, Dec. 1994.
- [103] M. Unser, P. Thévenaz, C. Lee, and U. E. Ruttimann, "Registration and statistical analysis of PET images using the wavelet transform," *IEEE Eng. in Med. and Biol.*, vol. 14, no. 5, pp. 603-611, 1995.
- [104] M. Vetterli and J. Kovacevic, *Wavelets and Subband Coding*. Englewood Cliffs, NJ: Prentice Hall, 1995.
- [105] D. Walnut, "Local inversion of the radon transform in the plane using wavelets," in *Proc. SPIE Conf. Wavelet Applicat. in Signal and Image Process.*, San Diego, CA, 1993, vol. 2034, pp. 84-91.
- [106] K. Wang and S. A. Shamma, "A functional model of the early auditory system," in *Proc. IEEE-SP Int. Symp. Time-Frequency and Time-Scale Analysis*, Victoria, BC, Canada, Oct. 1992, pp. 45-48.
- [107] —, "Auditory analysis of spectrotemporal information in acoustic signals," *IEEE Eng. in Med. and Biol. Mag.*, vol. 14, no. 2, pp. 186-194, 1995.
- [108] A. B. Watson, "The cortex transform: rapid computation of simulated neural images," *Computer Vision Graphics Image Process.*, vol. 39, no. 3, pp. 311-327, 1987.
- [109] J. B. Weaver and D. M. Healy, "Signal to noise ratios and effective repetition times for wavelet and adapted wavelet encoding," *J. Magnet. Reson.*, to be published.
- [110] J. B. Weaver, X. Yansun, D. M. Healy, Jr., and L. D. Cromwell, "Filtering noise from images with wavelet transforms," *Magnet. Reson. in Med.*, vol. 21, no. 2, pp. 288-295, 1991.
- [111] J. B. Weaver, X. Yansun, D. M. Healy, and J. R. Driscoll, "Wavelet-encoded MR imaging," *Magnet. Reson. in Med.*, vol. 24, no. 2, pp. 275-287, 1992.
- [112] Y. Xing, W. Huda, A. F. Laine, and J. Fan, "Simulated phantom images for optimizing wavelet-based image algorithms in mammography," in *Proc. SPIE Conf. Mathemat. Methods in Med. Imaging III*, 1994, vol. 2299, pp. 207-217.
- [113] Y. Xu, J. B. Weaver, D. M. Healy, Jr., and J. Lu, "Wavelet transform domain filters: A spatially selective noise filtration technique," *IEEE Trans. Image Process.*, vol. 3, pp. 747-758, Dec. 1994.
- [114] X. Yang, K. Wang, and S. A. Shamma, "Auditory representations of acoustic signals," *IEEE Trans. Informat. Theory*, vol. 38, pp. 824-839, Feb. 1992.
- [115] L. P. Yaroslavsky, "The theory of optimal methods for localization of objects in pictures," in *Progress in Optics*, E. Wolf, Ed. Amsterdam: Elsevier, pp. 145-201, 1993.
- [116] Y. Yoshida *et al.*, "Automated detection of clustered microcalcifications in digital mammograms using wavelet processing techniques," in *Proc. SPIE Conf. Med. Imag.*, 1994, vol. 2167.



Michael Unser (Senior Member, IEEE) was born in Zug, Switzerland, on April 9, 1958. He received the M.S. (summa cum laude) and Ph.D. degrees in electrical engineering from the Swiss Federal Institute of Technology, Lausanne, in 1981 and 1984, respectively.

In 1985, he joined the Biomedical Engineering and Instrumentation Program, National Institutes of Health, Bethesda, MD. His research interests include the application of image processing and pattern recognition techniques to various biomedical problems, multiresolution algorithms, wavelet transforms, and the use of splines in signal processing. He is the author of more than 50 published journal papers. He serves as an Associate Editor for the IEEE TRANSACTIONS ON IMAGE PROCESSING and the IEEE SIGNAL PROCESSING LETTERS and is on the editorial board of SIGNAL PROCESSING and PATTERN RECOGNITION.

Dr. Unser received the Dommer Prize for excellence from the Swiss Federal Institute of Technology in 1981, the research prize of the Brown-Bowery Corporation 1984, and the IEEE Signal Processing Society's 1995 Best Senior Paper Award (IMDSP technical area) for a TRANSACTIONS paper (with A. Aldroubi and M. Eden) on B-spline signal processing. He is a member of the Image and Multidimensional Signal Processing Committee of the IEEE Signal Processing Society.



Akram Aldroubi received the M.S. degree in electrical engineering from the Swiss Federal Institute of Technology, Lausanne, Switzerland, in 1982. He received the M.S. and the Ph.D. degrees in mathematics from Carnegie-Mellon University, Pittsburgh, PA, in 1984 and 1987, respectively.

He is currently a Staff Scientist at the Biomedical Engineering and Instrumentation Program, National Institutes of Health. His research interests include functional analysis, partial differential equations, wavelets, and signal/image processing.

Dr. Aldroubi is a member of the American Mathematical Society. He helped organize the 1994 IEEE-EMBS Workshop on *Wavelets in Medicine and Biology*, and SPIE's *Wavelet Applications in Signal and Image Processing IV*. He received the René Cousin prize for excellence from the Swiss Federal Institute of Technology in 1982, and the IEEE Signal Processing Society's 1995 Best Senior Paper Award (IMDSP technical area) for a TRANSACTIONS paper (with M. Unser and M. Eden) on B-spline signal processing.